The Quantum Monte Carlo Simulation of Transverse Field Ising Model

Yuanxing Duan, Shixin Hu, and Fangyu Xiong

School of Physics, Peking University

December 31, 2020

Abstract

Ising model is one of the most important models in the field of statistical mechanics. Despite its simplicity, it shows plenty of rich physics such as critical phenomena, and its relation to $\mathbb{Z}_2$ gauge theory. In this project, we use numerical Monte Carlo method, including the classical Metropolis and the so-called Worm algorithm to simulate the transverse field Ising model (TFI) in different spatial dimensions to reveal its critical behavior, such as its phase transition temperature, some critical exponents, as well as its critical dimension necessary to make the spontaneous symmetry breaking possible.

1 Introduction

Ising model is one of the most fundamental model in statistical mechanics. The ferromagnetic transverse field Ising model Hamiltonian is:

$$\mathcal{H} = -J\sum_{\langle ij\rangle}\sigma_i^z\sigma_j^z - h\sum_i \sigma_i^x \tag{1}$$

where σ_i^α are the Pauli matrices representing the αth component of the spin-1/2 on site i, and $J > 0$. When $h = 0$, corresponding to the classical Ising model, the eigenstates of this Hamiltonian are simply the direct product of the σ^z basis of all sites, and we can simply replace the Pauli matrices σ_i^z by their eigenvalues, which are either 1 or -1. When we turn on the transverse field h, quantum effects come in the story, since there will be fluctuations around the σ^z basis of the classical Ising model and basically the true eigenstates of the quantum Ising model with finite h will be an entangled state.

One of the main aspects that make Ising model so important in statistical mechanics is its thermodynamic fluctuation, especially its behavior near criticality. For simplicity, we let $h = 0$ and add a longitudinal field h_z in the discussion of thermodynamic behavior, so the Hamiltonian becomes

$$\mathcal{H} = -J\sum_{\langle ij\rangle}\sigma_i^z\sigma_j^z - h_z\sum_i \sigma_i^z. \tag{2}$$

From statistical mechanics, we can easily write down its partition function, and use different methods to solve the problem (transfer matrix for dimension $d = 1$, mean field for $d > 1$, as well as various numerical methods). We take $d = 2$ as an example to see its critical behavior. At first it has a finite critical temperature between

paramagnetic phase at higher temperature and ferromagnetic phase at lower temperature:

$$\sinh\left(\frac{2J}{T_c}\right) = 1, \tag{3}$$

$$T_c = \frac{2J}{\log(1+\sqrt{2})}. \tag{4}$$

The phase transition corresponds to a $\mathbb{Z}_2$ symmetry breaking. Next we can get different physical quantities with respect to temperature: Magnetization:

$$M = \langle \sigma_i^z \rangle \sim (T_c - T)^{\frac{1}{8}}. \tag{5}$$

Susceptibility:

$$\chi = \frac{\partial M}{\partial h_z} \sim (T - T_c)^{-\frac{7}{4}}, \tag{6}$$

and so on.

In particular, the two-point correlation function $\Gamma(i-j) = \langle \sigma_i^z \sigma_j^z \rangle - \langle \sigma_i^z \rangle \langle \sigma_j^z \rangle$ behave differently at different temperature. When T is away from T_c, the correlation function decay exponentially:

$$\Gamma(i-j) \sim e^{\frac{|i-j|}{\xi(T)}}, \tag{7}$$

with correlation length $\xi(T) \sim \frac{1}{|T-T_c|}$. As $T \to T_c$, the correlation length diverges, and the correlation function behaves like

$$\Gamma(i-j) \sim \frac{1}{|i-j|^{d-2+\eta}}. \tag{8}$$

The critical exponents are listed as Table 1.

Table 1: Critical exponents of the Ising model.

Exponents	Definition		Ising Value
α	C	$\propto (T-T_c)^{-\alpha}$	0
β	M	$\propto (T_c-T)^{\beta}$	1/8
γ	χ	$\propto (T-T_c)^{-\gamma}$	7/4
δ	M	$\propto h^{1/\delta}$	15
ν	ξ	$\propto (T-T_c)^{-\nu}$	1
η	$\Gamma(n)$	$\propto \lvert n\rvert^{2-d-\eta}$	1/4

Now let's see the case of quantum phase transition, where we turn on the transverse field h and let $h_z = 0$, so we go back to the original Hamiltonian. We may analyse the behavior of the system at the first glance as we vary h. For $h < h_c$, with h_c the critical field, the classical Ising interaction is the leading term, so the spin tend to be aligned in the z direction, resulting in the ordered phase in S_z representation, while in the S_x representation the phase will be disordered. On the other hand, for $h > h_c$, the spin tend to polarized in x direction, so we may get the phase with ordered S_x and disordered S_z. This shows the implicit duality between S_x and S_z representation.

In order to calculate the properties of quantum criticality such as the correlation functions more conveniently, we start from Jordan-Wigner transformation in one dimensional system:

$$\sigma_i^z = -\prod_{j<i}(1 - 2c_j^\dagger c_j)(c_i + c_i^\dagger) \tag{9}$$

$$\sigma_i^x = 1 - 2c_i^\dagger c_i \tag{10}$$

with $c_i, c_i^\dagger$ the creation and annihilation operators of fermion. Correspondingly the Hamiltonian can be expressed as:

$$\mathcal{H} = -J\sum_i (c_i^\dagger c_{i+1} + c_{i+1}^\dagger c_i + c_i^\dagger c_{i+1}^\dagger + c_{i+1} c_i) - h\sum_i (1 - 2c_i^\dagger c_i) \tag{11}$$

We may diagonalize this Hamiltonian via Bogoliubov transformation just like what we do in spin wave theory and BCS superconductors. If we further introduce the Majorana fermion representation:

$$i\psi_i = c_i - c_i^\dagger \tag{12}$$

$$\bar{\psi}_i = c_i + c_i^\dagger \tag{13}$$

and do the Wick rotation to the imaginary time, we may get the action of the free Majorana fermion (in the continuous limit):

$$S = \frac{i}{2}\int \psi(\partial_0 - \partial_1)\psi + \bar{\psi}(\partial_0 + \partial_1)\bar{\psi} + m_0\psi\bar{\psi} \tag{14}$$

where $\partial_0 = \partial_t, \partial_1 = \partial_x$, and $m_0 = 1 - h/J$. When $h = J$, we reached the criticality with scale invariance. The corresponding correlation functions are:

$$\langle \sigma_i^z(i)\sigma_i^z(i+n)\rangle \sim \frac{1}{|n|^{1/4}} \tag{15}$$

$$\langle \sigma_i^x(i)\sigma_i^x(i+n)\rangle \sim \frac{1}{|n|^2} \tag{16}$$

Then we show the relation between classical and quantum model. If we take $\beta = 1/kT$ as imaginary time, we can calculate the partition function $\mathcal{Z} = \mathrm{Tr}[e^{-\beta H}]$ by path integral approach:

$$\begin{aligned}\mathcal{Z} = \sum_{\{S_{i,l}^z\}} &\left\langle \left\{S_{i,1}^z\right\} \middle| e^{-\Delta\tau H} \middle| \left\{S_{i,L}^z\right\}\right\rangle \left\langle \left\{S_{i,L}^z\right\} \middle| e^{-\Delta\tau H} \middle| \left\{S_{i,L-1}^z\right\}\right\rangle \\ &\times \cdots \left\langle \left\{S_{i,2}^z\right\} \middle| e^{-\Delta\tau H} \middle| \left\{S_{i,1}^z\right\}\right\rangle\end{aligned} \tag{17}$$

where all $S_{i,l}^z$ are $\mathbb{Z}_2$ variables representing z-components of spins at site i and time index l. The time slice $\Delta\tau = \beta/L$ and $L \to \infty$. After some calculation, we get the following partition function:

$$\mathcal{Z} = \Lambda^{NL}\sum_{\{S_{i,l}^z\}} \exp\left[\sum_{i=1}^{N}\sum_{l=1}^{L}\left(\Delta\tau J S_{i,l}^z S_{i+1,l}^z + \gamma S_{i,l}^z S_{i,l+1}^z\right)\right] \tag{18}$$

with $\gamma = -\frac{1}{2}\log[\tanh(\Delta\tau h)]$ and $\Lambda^2 = \sinh(\Delta\tau h)\cosh(\Delta\tau h)$. So we can see that the $1+1$ dimensional quantum Ising model is mapped to a $2+1$ dimensional classical Ising model. Moreover, when we vary the transverse field h, the system will exhibit quantum phase transition.

2 Worm Algorithm

The Hamiltonian of quantum transverse-field Ising model (TFI) can be rewritten as

$$\mathcal{H} = -t\sum_{\langle ij\rangle}\sigma_i^x\sigma_j^x - h\sum_i \sigma_i^z = K + U. \tag{19}$$

And the interaction term K can be further expressed in terms of the raising and lowering operators as

$$K = K_1 + K_2 = -t\sum_{\langle ij\rangle}(\sigma_i^+\sigma_j^- + \text{h.c.}) - t\sum_{\langle ij\rangle}(\sigma_i^+\sigma_j^+ + \text{h.c.}). \tag{20}$$

Then with the Holstein-Primakoff transformation $b_i(b_i^\dagger) = \sigma_i^+(\sigma_i^-)$ and $n_i = b_i^\dagger b_i = (\sigma_i^z + 1)/2$, the TFI can be mapped onto a Bose-Hubbard (BH) model whose Hamiltonian is

$$\mathcal{H} = -t\sum_{\langle ij\rangle}(b_i^\dagger b_j + \text{h.c.}) - t\sum_{\langle ij\rangle}(b_i^\dagger b_j^\dagger + \text{h.c.}) - \mu\sum_i n_i, \tag{21}$$

where the chemical potential $\mu = 2h$. For this BH model, K_1 accounts for the hopping of a particle, and K_2 simultaneously creates or deletes a pair of nearest neighbouring (NN) particles.

We can use the imaginary-time path integral to represent the partition function:

$$\mathcal{Z} = \text{Tr}\left(\mathrm{e}^{-\beta\mathcal{H}}\right) = \sum_{\alpha_0}\langle\alpha_0|\,\mathrm{e}^{-\beta\mathcal{H}}\,|\alpha_0\rangle \tag{22}$$

$$= \lim_{\mathrm{d}\tau=\frac{\beta}{n},n\to\infty}\sum_{\{\alpha_i\}}\langle\alpha_0|\,\mathrm{e}^{-\mathcal{H}\mathrm{d}\tau}\,|\alpha_{n-1}\rangle\cdots\langle\alpha_i|\,\mathrm{e}^{-\mathcal{H}\mathrm{d}\tau}\,|\alpha_0\rangle \tag{23}$$

$$= \sum_{\alpha_0}\sum_{\mathcal{N}}^{\infty}\int_0^\beta\int_{\tau_1}^\beta\cdots\int_{\tau_{\mathcal{N}-1}}^\beta\prod_{k=1}^{\mathcal{N}}\mathrm{d}\tau_k\,F(t,h), \tag{24}$$

with the integrand function

$$F(t,h) = t^{\mathcal{N}_h+\mathcal{N}_p}\mathrm{e}^{-\int_0^\beta U(\tau)\,\mathrm{d}\tau}, \tag{25}$$

where $\mathcal{N}_h$ and $\mathcal{N}_p$ are the number of hopping and pairing kinks. So the partition function $\mathcal{Z}$ can be regarded as the summation of different configuration in the $(d+1)$D space-time, of which the statistical probability is

$$W_{\mathcal{Z}}(t,h) = \prod_{k=1}^{\mathcal{N}}\mathrm{d}\tau\,F(t,h). \tag{26}$$

In this representation, each configuration can be viewed in the following way. For each lattice site i, the spin σ_i^z may be flipped by the hopping or pairing at some imaginary time τ_k. Since either hopping or pairing term simultaneously flips spins at two NN sites, so one can construct a loop by following the spin-up segments along the imaginary time, and kinks which labels the spin flips of two NN sites. Hence, a configuration can be identified with several loops of spin-up in the $(d+1)$D space-time.

Then, we can extend the configuration space $\mathcal{Z}$ to $\mathcal{G}$ by including two defects, which corresponds to the spin-spin correlation function:

$$\mathcal{G}(\boldsymbol{x}_I,\tau_I;\boldsymbol{x}_M,\tau_M) = \text{Tr}\left[T_\tau\left(\sigma_I^x(\tau_I)\sigma_M^x(\tau_M)\mathrm{e}^{-\beta\mathcal{H}}\right)\right], \tag{27}$$

where T_τ is the τ-ordering operator. In the configuration space $\mathcal{G}$, each configuration can be viewed as several loops and an open path with two ending points "Ira" (I) and "Masha" (M), which correspond to the two spins in the correlation function. Similarly, the statistical weight of the $\mathcal{G}$ configuration can be written as

$$W_{\mathcal{G}} = \frac{\mathrm{d}\tau_I\mathrm{d}\tau_M}{\omega_G}\prod_{k=1}^{\mathcal{N}}\mathrm{d}\tau_k\,F(t,h), \tag{28}$$

here ω_G is an arbitrary positive number. And when I coincides with M, the open path forms a loop, the configuration in the $\mathcal{G}$ space turns into one in the $\mathcal{Z}$ space.

The key idea of the worm algorithm is to move the defects I and M of the open path (like a worm wriggling) to produce different $\mathcal{G}$ and $\mathcal{Z}$ configurations for sampling. For ergodicity, the simulation should be able to change the number of kinks, the space-time location of kinks, and that of the defects I and M. So we perform the following three kinds of updates:

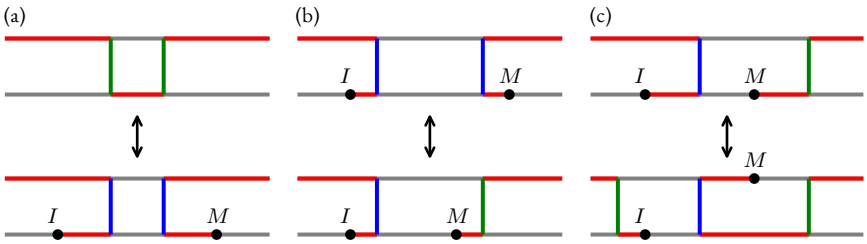

Figure 1: Three different kinds of updates. The red (gray) line denotes spin-up (spin-down) states, and the green (blue) line denotes hopping (pairing) kinks. (a) Create/annihilate defects I and M. (b) Move imaginary time of defect M. (c) Insert/delete a kink.

1. *Create/annihilate defects I and M.* If the current configuration is in the $\mathcal{Z}$ space, then "creating defects" is the only possible update. We randomly picks up a point $(\boldsymbol{x}_I, \tau_I)$ in the whole space-time, draws a uniformly distributed time displacement $\delta \in [-\tau_a/2, \tau/2]$ and $\delta \neq 0$, assigns $\boldsymbol{x}_M = \boldsymbol{x}_I$ and $\tau_M = \mathrm{mod}(\tau_I + \delta, \beta)$, and flips the spin state between I and M.

   The reverse operation of "creating defects" is "annihilating defects", which is chosen with an *a priori* probability $\mathcal{A}_a$ in the $\mathcal{G}$ space. By annihilating defects I and M and flipping the spin state in-between, a $\mathcal{G}$ configuration are changed into a $\mathcal{Z}$ configuration. The annihilation is possible only if I and M are on the same world line $\boldsymbol{x}_I = \boldsymbol{x}_M$ and their imaginary-time displacement $\min\{|\tau_I - \tau_M|, \beta - |\tau_I - \tau_M|\} \leq \tau_a/2$.

   The detailed-balance condition of creating and annihilating defects reads as

$$\frac{\mathrm{d}\tau_I}{\beta N}\frac{\mathrm{d}\tau_M}{\tau_a} \cdot W_{\mathcal{Z}} \cdot \mathcal{P}_{\mathrm{crea}} = \mathcal{A}_a \cdot W_{\mathcal{G}} \cdot \mathcal{P}_{\mathrm{anni}}, \tag{29}$$

   which leads to the acceptance probabilities

$$P_{\mathrm{crea}} = \min\left[1, \mathcal{A}_a \tau_a \frac{\beta N}{\omega_G}\frac{F_{\mathrm{new}}}{F_{\mathrm{old}}}\right], \tag{30}$$

$$P_{\mathrm{anni}} = \min\left[1, \frac{1}{\mathcal{A}_a \tau_a}\frac{\omega_G}{\beta N}\frac{F_{\mathrm{new}}}{F_{\mathrm{old}}}\right], \tag{31}$$

   where F_{old} and F_{new} are given by Eq. 25. And here we choose $\omega = \beta N$ to make the calculation simpler.

2. *Move imaginary time of defect M.* This kind of update is chosen with a probability $\mathcal{A}_b$ in the $\mathcal{G}$ space. We randomly select a imaginary-time displacement $\delta \in [-\tau_b/2, \tau_b/2]$ and $\delta \neq 0$, assigns $\tau'_M = \mathrm{mod}(\tau_M + \delta, \beta)$ for the new temporal location of defect M, and flips the spin states in-between. The acceptance probability is

$$P_{\mathrm{move}} = \min\left\{1, \frac{F_{\mathrm{new}}}{F_{\mathrm{old}}}\right\}. \tag{32}$$

3. *Insert/delete a kink.* Each operation is chosen with a probability $\mathcal{A}_c$ in the $\mathcal{G}$ space. When "inserting a kink", we randomly choose one of the $z_d = 2d$ neighbouring world lines of $\boldsymbol{x}_M$, denote it as $\boldsymbol{x}'_M$, and updates the location of M from $(\boldsymbol{x}_M, \tau_M)$ to $(\boldsymbol{x}'_M, \tau_M)$. Meanwhile, we insert a kink k between world lines $\mathbf{x}_M$ and $\mathbf{x}'_M$ at imaginary time $\tau_k = \mathrm{mod}(\tau_M + \delta, \beta)$, with a random displacement $\delta \in [-\tau_c/2, \tau_c/2]$ and $\delta \neq 0$. Further, the spin states between τ_M and τ_k, on both $\mathbf{x}_M$ and $\mathbf{x}'_M$, are flipped.

   In the reverse operation, "deleting a kink", we also pick up a random neighbouring world line $\mathbf{x}'_M$ of $\mathbf{x}_M$ and moves M from $(\mathbf{x}_M, \tau_M)$ to $(\mathbf{x}'_M, \tau_M)$. If there is no kink that connects world lines $\mathbf{x}_M$ and $\mathbf{x}'_M$ in the imaginary-time domain $[\tau_M - \tau_c/2, \tau_M + \tau_c/2]$, the operation is rejected. Otherwise, we randomly

pick up one of those n_k in this region and delete it, and meanwhile flip the spin states on both world lines between τ_M and the imaginary time of the deleted kink.

The detailed balance condition of this pair of operations is

$$\mathcal{A}_c \cdot \frac{1}{z_d} \cdot \frac{\mathrm{d}\tau}{\tau_c} \cdot W \cdot \mathcal{P}_{\text{inse}} = \mathcal{A}_c \cdot \frac{1}{z_d} \cdot \frac{1}{n_k} \cdot W_+ \cdot \mathcal{P}_{\text{dele}}, \tag{33}$$

which leads to the acceptance probabilities

$$P_{\text{inse}} = \min\left[1, \frac{\tau_c}{n_k+1}\frac{F_{\text{new}}}{F_{\text{old}}}\right], \tag{34}$$

$$P_{\text{dele}} = \min\left[1, \frac{n_k}{\tau_c}\frac{F_{\text{new}}}{F_{\text{old}}}\right]. \tag{35}$$

The worm algorithm can be concluded as Algorithm 1, in which *a priori* probabilities satisfy $\mathcal{A}_a + \mathcal{A}_b + 2\mathcal{A}_c = 1$.

Algorithm 1 Worm algorithm

```
initialization;
thermalization;
loop
  if it is a 𝒵 configuration then
    compute statistical quantities of this configuration;
    choose the "creating defects (I, M)" operation;
  else
    choose an operation with its a priori probability; except "creating defects (I, M)";
  end if
  calculate the acceptance probability P and carry out the operation with the probability P;
end loop
```

3 Numerical Results

We calculate the phase transition of TFI based on the worm algorithm. When the transverse field $h = 0$, there exists the $\mathbb{Z}_2$ symmetry which means that the spin-up and spin-down states are fully balanced, and the system is in a ferromagnetic phase. As h turns on, the system evolves into a disordered phase with the spin-down state being suppressed. And once $h > h_c$, the system enters into the spin-up ordered phase through a second-order quantum phase transition. Because it is h_c/t rather than h_c itself that describes the physical properties of the model, we simply set $t = 1$ for simplicity of calculation.

We discretize the imaginary time so that the calculation is more efficient, which makes our system is indeed a $(d+1)$D lattice. Because the dynamic critical exponent $z = 1$ for the TFI, we choose the inverse temperature $\beta = L$, where L is the spatial lattice size. We also applied the periodic boundary conditions, so the space-time lattice is a torus in fact. We mainly calculate the 1D TFI with $L = 64$ and 128 in our current work.

In Fig. 2 we show typical $\mathcal{Z}$ configurations when $h = 0.01, 0.5, 1.0, 1.5$. It is obvious that when $h < 1$, there are many loops wrapping around the spatial direction; but when $h > 1$, the loops are small and unable to percolate.

To get the critical point h_c, we mainly focus on the topological properties instead of physical quantities like the magnetic susceptibility of $\mathcal{Z}$ configurations when sampling. In more detail, for a given $\mathcal{Z}$ configuration, we

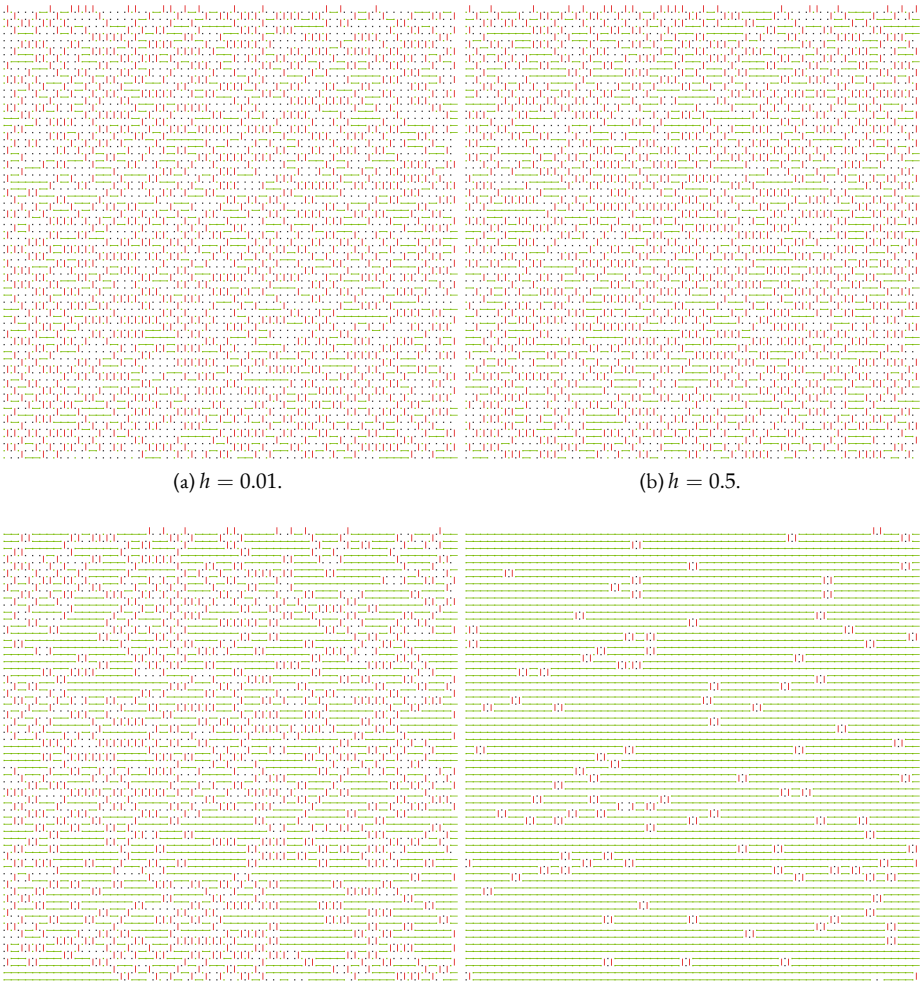

(a) $h = 0.01$. (b) $h = 0.5$.

(c) $h = 1.0$. (d) $h = 1.5$.

Figure 2: Typical $\mathcal{Z}$ configurations when the transverse field h is different. The spatial direction is vertical and the imaginary time direction is horizontal. The black (green) dots represent the spin-up (spin-down) states, and the red lines represents two kinds of kinks.

can count the winding number W_i^l of the l-th loop along the i-th spatial direction. The total winding number $W_i = \sum_l W_i^l$ can be used to determine whether the $\mathcal{Z}$ configuration wrap along the i-th direction or not, which is indicated as $R_i = 1$ if $W_i > 0$ and $R_i = 0$ otherwise. Then the average wrapping probability $R = \sum_{i=1} \langle R_i \rangle / d$ is calculated, which indicates whether the in-site energy U or the interaction K dominates. If $|h| \gg 1$, U dominates, which means that the loops are small and difficult to percolate, hence R should be small (near 0). But if $|h| \ll 1$, K dominates, so R should be large (near 1). In calculation, we traverse all loops of a $\mathcal{Z}$ configuration based on depth-first search (DFS).

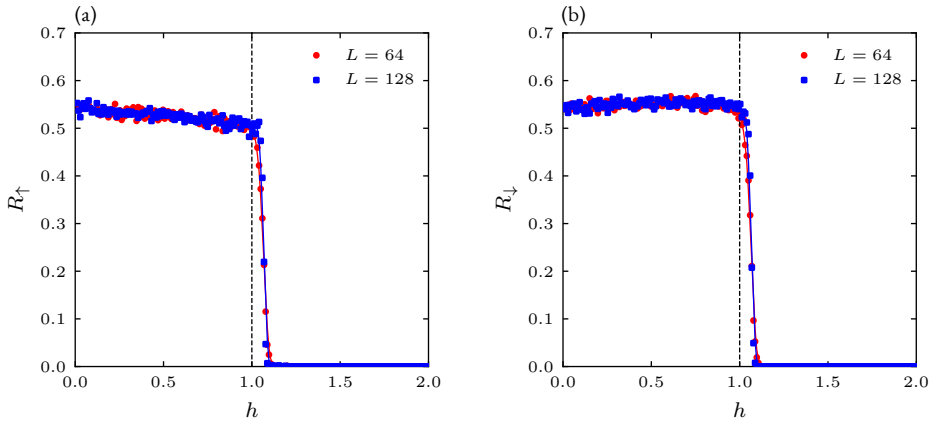

Figure 3: Wrapping probabilities $R_\uparrow$ and $R_\downarrow$ versus the transverse field h. (a) Spin-up. (b) Spin-down.

The Monte Carlo results in Fig. 3 show that both the spin-up and spin-down loops display critical behaviors near $h = h_c = 1$, which is the theoretical value of the critical point. When $h < h_c$, $R_\uparrow$ and $R_\downarrow$ have non-zero values, which means the system is indeed in an interaction-dominating phase. When h increases, $R_\uparrow$ slowly decreases, which is easy to understand, since the increasing h makes $\mathcal{Z}$ configurations with "longer fragments" of spin-up states for a given lattice site along the imaginary time direction are more possible to be sampled, which slightly restrains the wrapping probability of spin-up. For a similar reason, $R_\downarrow$ increases slightly when h increases. If h increases further over h_c, $R_\downarrow$ will drop to 0 quickly, since the spin-down loops are too small to wrap around the spatial direction. The same behavior is seen for $R_\uparrow$, which is because in this phase, most sampled $\mathcal{Z}$ configurations will be dominated by spin-up states, which makes the number of kinks too small for spin-up loops to percolate.

We also calculate the correlation functions C_n of this system, which is defined as:

$$\overline{\sigma_i^z} \equiv \frac{1}{L^2} \sum_{j,k} \sigma_{j,k}^z, \tag{36}$$

$$\overline{\sigma_i^z \sigma_{i+n}^z} \equiv \frac{1}{L^2} \sum_{j,k} \sigma_{j,k}^z \sigma_{j+n,k}^z, \tag{37}$$

$$C_n \equiv \overline{\sigma_i^z \sigma_{i+n}^z} - \overline{\sigma_i^z}^2, \tag{38}$$

where $\sigma_{j,k}^z$ is the spin state at site j and imaginary time k. Fig. 4 shows that when $L = 64$ and 128, these quantities also indicate the existence of phase transition and criticality. We notice that these quantities show little dependence on the lattice size L, which is reasonable since the lattice sizes we used in calculation are not so small. However, the finite-size effect can also be seen in the results, which eliminates the divergence of C_1 at the critical point. Moreover, the peaks of C_1 in Fig. 4 are a bit lager than h_c. We think this comes from the influences of the finite-size effect and the non-zero temperature $\beta = L < \infty$.

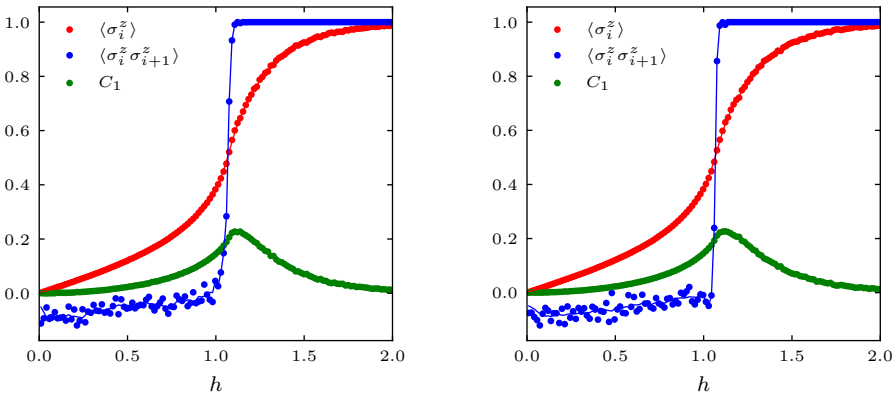

Figure 4: Expectation values of spin states $\overline{\sigma_i^z}$, product of NN spins $\overline{\sigma_i^z\sigma_{i+1}^z}$ and correlation function C_1 versus transverse field h. (a) $L = 64$. (b) $L = 128$.

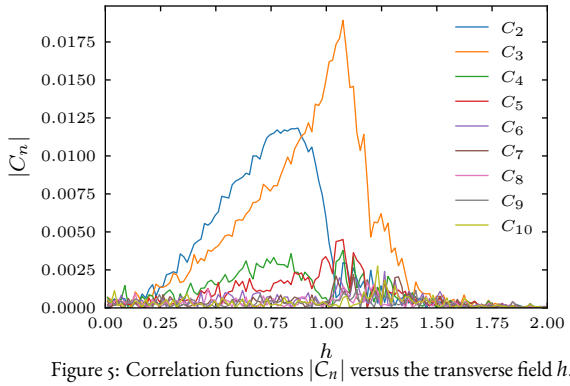

Figure 5: Correlation functions $|C_n|$ versus the transverse field h.

Different correlation functions $|C_n|$ with different transverse field h are shown in Fig. 5. We see that there are peaks of $|C_n|$ when h is near h_c. This is also consistent with the phase transition. However, we notice that the positions of peaks of different $|C_n|$ are not the same. More precisely, it seems that the peaks of $|C_{2n}|$ and those of $|C_{2n+1}|$ are at two distinct positions. We do not quite understand this behavior, which may give insights to more interesting correlation effects in TFI.

We are sorry that we didn't calculate many of the physical quantities that we wrote in our project plan. The time limitation is the major cause of it. Because we find that using worm algorithm to solve TFI is a completely different project to solving the classical Ising model, and it's more interesting and adventurous, so we focused on this. We planned to write code for different dimensional TFI, but since the code is highly relevant to the dimensionality (data structures, traverse methods, etc.), we didn't have time to implement another version of code. And some data are not so satisfactory due to the limitation of computational resource. Nevertheless, we think the worm algorithm, which ingeniously combines the Monte Carlo method and the path integral approach, has high efficiency which makes it possible to use this algorithm to solve many more complex problems.

Contributions

- Yuanxing Duan:
  1. Understanding and realizing the worm algorithm, debugging and optimizing the C++ code that used to generate data.
  2. Running the code on his own machine, Ryzen R9 3950x.
  3. Visualization (Fig. 2).
- Shixin Hu:
  1. Theoretical analysis and some predictions on the critical behavior of correlation functions (Sec. 1).
  2. Report writing of the Introduction part (Sec. 1).
- Fangyu Xiong:
  1. Helping Yuanxing Duan in understanding the worm algorithm, designing of the algorithm to compute the wrapping probability, and determining what quantities to calculate.
  2. Writing Sec. 2-3 of the report.
  3. Plotting Fig. 1,3-5. Making Table 1.
  4. Data analysis (Sec. 3).